Quantum Electronics **36** (2) 117 – 124 (2006)

INTERACTION OF LASER RADIATION WITH MATTER. LASER PLASMA

PACS numbers: 61.25.Em; 62.50.+p; 81.20.Ym
DOI: 10.1070/QE2006v036n02ABEH013113

Role of a dissolved gas in the optical breakdown of water

N.F. Bunkin, S.I. Bakum

Abstract. **It is shown experimentally that the optical breakdown in water produced by nanosecond pulses is initiated by a gas dissolved in it due to the formation of bubston clusters playing the role of heterogeneous seeds of the breakdown. By using the method proposed in the paper, a completely degassed water is obtained, which is optically stable to the seed mechanism of breakdown both away and near the boiling point. The existence of long-lived hydrates of a dissolved gas in water is established and a new effect of water purification from such hydrate traps by 'washing' it with helium is discovered.**

Keywords: *optical breakdown, interaction of radiation with matter, optical breakdown mechanism.*

1. Introduction: Optical breakdown mechanisms

It was pointed out in many experimental papers that the optical breakdown in liquids (at least by nanosecond laser pulses) occurs sporadically, appearing not at each laser pulse. In addition, the breakdown takes place not only in the focus of a lens but can appear both in front of the beam waist and behind it. When long-focus lenses are used, the breakdown acquires the so-called multiple character, each flash consisting of individual microflashes (Fig. 1). It is found that the breakdown threshold increases after careful purification of a liquid. The spectrum of the optical-breakdown flash is continuous (it has no characteristic lines), which is inherent in thermal radiation. Based on these data, it was assumed that the breakdown is initiated by absorbing solid microimpurities (see, for example, review [1]). The breakdown threshold also very weakly depends on the laser radiation wavelength. This led to a conclusion that the breakdown is initiated by particles absorbing light in a very broad spectral range, in particular, by soot particles [2]. However, this model is not devoid of contradictions. Thus, in many experiments a breakdown was observed even in very carefully purified liquids (for example, purified by using the Milli-pore technology removing particles of size no less than 100 nm). In addition, the presence of absorbing microparticles in the focus of a lens should result in the heating of caustic and efficient thermal defocusing, i.e., the conditions for breakdown initiation should get worse upon 'contamination' of the liquid by absorbing impurities. Thus, we found in our experiments [3] that under the invariable focusing conditions and parameters of the laser pulse, the breakdown disappeared during a gradual addition of micron activated coal particles into water preliminary purified in a Milli-pore unit. We also determined the dependence of the breakdown threshold on the cell height and showed that the breakdown had the seed nature and the seed density decreased with increasing the depth of a liquid layer [3].

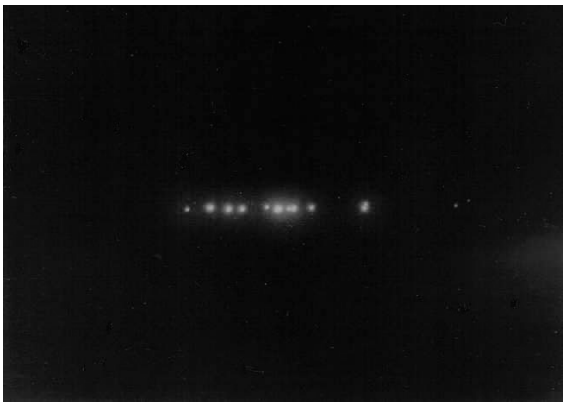

Figure 1. Picture of the multiple breakdown of water irradiated by a 50-ns pulse obtained with an optical microscope.

The alternate mechanism of breakdown in liquids assumes that the breakdown occurs as in amorphous semiconductors (with some reservations). According to this mechanism, an electron avalanche develops in a liquid irrespective of the presence of seeds in it. The liquid breakdown model based on these concepts has become quite popular (see review [4] and references therein). Review [4] is entirely devoted to the optical breakdown in water, assuming that water is a semiconductor with an energy gap of 6.5 eV. This value of the energy gap was taken from experimental papers [5, 6] in which water was treated as an amorphous semiconductor.

It is obvious that for such an energy gap and wavelengths in the optical spectral range, the electron avalanche

N.F. Bunkin Scientific Center for Wave Studies, A.M. Prokhorov General Physics Institute, Russian Academy of Sciences, ul. Vavilova 38, 119991 Moscow, Russia; e-mail: nbunkin@kapella.gpi.ru
S.I. Bakum N.S. Kurnakov Institute of General and Inorganic Chemistry, Russian Academy of Sciences, Leninsky prosp. 31, 117907 Moscow, Russia

Received 10 August 2005; revision received 5 December 2005
Kvantovaya Elektronika **36** (2) 117 – 124 (2006)
Translated by M.N. Sapozhnikov

can appear only due to multiphoton ionisation. The authors of [4] assume that the theoretical results obtained in [7] for the multiphoton ionisation of semiconductors can be also applied to liquid water. In our opinion, this model of the optical breakdown of liquids is also not devoid of disadvantages because the derivation of the dynamic equation for the electron density neglects losses caused by the attachment of electrons to adjacent molecules and recombination between electrons and positive ions. The only mechanism of electron-density losses considered in this case is the diffusion of electrons from the caustic.

Thus, this approach is valid if the breakdown occurs during times shorter than the lifetime τ of a hydrated electron, which is very short, lying in the range $1-1.5$ ps (see, for example, monograph [8] and references therein). Such a short lifetime of a hydrated electron is obviously explained by capturing this electron by surrounding water molecules. In other words, the optical breakdown model proposed in [4] can be applied if only electrons have time to acquire a sufficient energy before they will be captured by surrounding water molecules. This requires the pulse duration τ_p shorter than τ, i.e., the electron should have time to acquire the energy that is sufficient not only for a 'detachment' from the water molecule but also for ionisation of other water molecules and the initiation of the electron avalanche. If the condition $\tau_p < \tau$ is not fulfilled, the dynamic equation for the density of electrons produced upon multiphoton ionisation should be derived by taking into account losses caused by the electron dipole and electron–ion interactions.

Note that review [4] presents the results of various experiments in which the pulse duration was varied from 30 ns to 100 fs and the breakdown threshold intensities were in the range from 10^9 to 10^{12} W cm^{-2}. Most likely this approach, indeed, can be used in the case of femtosecond pulses for intensities of about 10^{12} W cm^{-2}. However, it is doubtful that this model is valid for all experiments described in [4] (this concerns especially nanosecond pulses with intensities of the order of 10^9 W cm^{-2}).

We are not going to dispute here with the authors of review [4], although the results of experiments presented in it substantially differ from the results of our papers (see below). We assume that our experiments and those described in [4] are related to different breakdown regimes. For example, the possibility of a multiple breakdown is nowhere mentioned in [4], whereas we always observed such a breakdown in our experiments (Fig. 1). In addition, the possibility of a sporadic breakdown was pointed out both in our papers and [4], but with substantial differences. In [4], the sporadic regime appears only when impurities are added into an initially pure liquid, which, being in the focal region, are easily ionised and 'supply' seed electrons, i.e., in this case the multiphoton ionisation of molecules of the liquid itself is not required, whereas in our experiments the sporadic regime appears in a carefully purified liquid, from which all external impurities were preliminary removed (see details below).

Finally, in [4] the plasma region formed upon breakdown occupies the entire caustic volume (as upon the breakdown of gases). In this case, laser radiation is completely screened, i.e., the breakdown plasma completely absorbs radiation and radiation is absent behind the breakdown region. Note that the latter circumstance is especially substantial for the authors of [4] because their review is devoted to the application of laser radiation in ophthalmology where the locality of the laser action is very important (laser radiation should be reliably completely absorbed by the breakdown plasma, never reaching the eyeground). At the same time, we never obtained the entire screening of radiation by the breakdown plasma in our experiments; according to our estimates, only approximately 5 % of the laser pulse energy was absorbed during breakdown.

The review of the literature presented here does not pretend, of course, to be complete, and this was not our aim. Note, however, that after the advent of ultrashort-pulse lasers, it became possible to observe new effects during optical breakdown. In this connection we mention experiments [9] on excitation of the optical breakdown in water by focused femtosecond pulses, which was accompanied by the beam filamentation, the breakdown threshold being substantially dependent on self-focusing conditions.

The aim of our paper is to refine the mechanism of optical breakdown of carefully purified water by nanosecond laser pulses taking into account the specific properties of such a breakdown such as its sporadic and multiple nature and the absence of the complete screening of radiation by the breakdown plasma. It is obvious that such mechanism cannot be caused by the presence of solid miroimpurities in water (which were removed preliminary). In addition, for the reasons presented above, we believe that the breakdown is not caused by the electron avalanche in the liquid itself. However, we assume that the electron avalanche can appear in a cavity filled with a gas in the liquid. The breakdown occurs inside such a cavity as in gases (see, monograph [10]). A free electron in the gas oscillates in the electric field of an optical wave along the electric field vector and acquires the energy $E = \hbar\omega/2$ (we consider one-photon excitation of the electron). If the electron is not subjected to collisions, this energy is maximal. If it collides with other particles, each collision changes the direction of electron motion with respect to the electric field vector and the electron again oscillates under the action of the optical wave. Therefore, the electron is efficiently heated during collisions and acquires finally the ionisation energy, resulting in the creation of the electron avalanche.

Turning to the problem of optical breakdown in water produced by nanoseconds laser pulses, note that the breakdown threshold in a gas at the atmospheric pressure is one-two orders of magnitude higher than the breakdown threshold in water. In addition, the spectrum of a breakdown flash in a gas is discrete and contains characteristic lines of atoms of this gas, whereas this spectrum in liquids is continuous. Therefore, it would be erroneous to simply extend the theory of breakdown in gases [10] to liquids.

To explain the specific features of optical breakdown in liquids, we have introduced the concept of a 'bubston' [11–13]. A bubston (bubble stabilised by ions) is a stable gas bubble in a liquid, which has the ion conductivity and is in equilibrium with the surrounding gas medium. According to our estimates, the bubston radius in water is 14 nm. Because the bubston is compressed by surface tension forces, a mechanism compensating for these forces and thereby providing the mechanical and diffusion equilibrium of the bubston (with respect to a gas dissolved in a liquid) should exist.

This mechanism is the selective adsorption of ions of the same sign on the liquid–gas surface, which provides a stable mechanical equilibrium between the surface tension pressure

and negative (stretching) pondermotive pressure caused by the Coulomb repulsion of adsorbed ions, i.e., the bubble is indeed stabilised by ions. It is shown that in the case of mechanical stability, the diffusion equilibrium between the dissolved and free gas inside the bubston (the equality of chemical potentials) also appears.

The presence of bubstons in carefully purified water was confirmed in experiments on small-angle scattering of slow neutrons [14] and laser [15, 16] and acoustic [17] cavitation. It was shown in [13] that bubstons are capable of coagulation with the formation of bubston clusters. According to our estimates, confirmed experimentally, the size of a bubston cluster is 1 – 1.5 μm. Such clusters can be observed by small-angle scattering of laser radiation [18 – 20]. A theoretical model describing the interaction of optical radiation with bubston clusters was developed [21], which was later confirmed in a number of experimental papers [22 – 24].

Now, we assume that each bubston of the bubston cluster contains a primary electron (the problem of a primary electron always exists, outside the context of the given task, therefore we will not discuss the reason for its appearance). The electron oscillates in the field of an optical wave as in the gas phase. However, one should take into account that the electron mean free path in gases at the atmospheric pressure is ~ 1 μm, whereas the bubston radius is 10 – 20 nm. Therefore, the electron is heated due to collisions not with gas molecules but with bubston walls, this heating occurring faster than in gases. Therefore, the hypothesis of bubston clusters as the seeds of optical breakdown explains the difference in the breakdown thresholds in gases and liquids.

The model considered in [21] assumes that collisions of electrons with a liquid wall are elastic. However, the model takes into account a decrease in the amount of electrons due to their attachment to a liquid wall resulting in the presence of the breakdown threshold. When the electron energy achieves the surface ionisation energy of a liquid (note that we used the ionisation potential of water equal to 6 eV, i.e., approximately the same value as in review [4]), the electron avalanche begins from liquid walls of a bubston. In this case, in each bubston the electron temperature (which 'breaks off' from the temperature of the surrounding liquid) and electron pressure drastically increase. In this regime, the walls between individual bubstons are evaporated and a macroscopic gas bubble of size ~ 1 μm is formed. We called this phenomenon the stimulated optical coalescence; it was later discovered experimentally in [25].

Upon irradiation by nanosecond pulses, stimulated optical coalescence appears already at the leading edge of the pulse; therefore, the pulse continues until coalescence termination, and electron oscillations are excited by the optical wave already inside a macroscopic bubble filled with heavy particles – molecules of the liquid ('fragments' of the liquid walls of a bubston cluster). Electrons collide with these particles, but now these collisions are inelastic: the electrons impart their momentum to particles and slow down (are 'cooled') by emitting bremsstrahlung radiation. Therefore, this approach allows one to explain the continuous spectrum of the optical breakdown flash in liquids. The breakdown flash is accompanied by a sound clap and the appearance of a macroscopic bubble, which experiences one-two pulsations and collapses. Therefore, the most specific features of the optical breakdown can be naturally explained within the framework of the model proposed in [21].

Finally, this model confirms the possibility of the sporadic and multiple character of the optical breakdown. Namely, for the given size of bubston and the given wavelength, the threshold radiation intensity I_{th} is calculated at which the electron energy achieves the energy of surface ionisation of bubston walls and the electron avalanche appears inside an individual bubston. Then, the concept of the breakdown volume V is introduced. This volume consists of two light cones directed toward each other with the caustic between them; the radiation intensity inside this volume is not lower than I_{th}. Obviously the volume V is determined by the pulse energy and focusing conditions, i.e., it can be calculated from the specified parameters of the laser beam. Therefore, if a cluster inside this volume comes to the laser beam during the laser pulse, a breakdown will occur (see Figs 1 and 2). One can see from Fig. 2 that the breakdown appears not necessarily in the caustic, i.e., the incident radiation is not screened by the breakdown plasma.

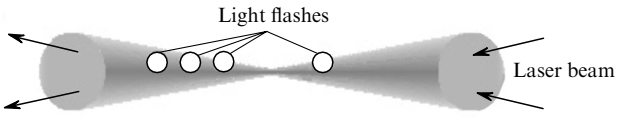

Figure 2. Scheme of excitation of an optical breakdown inside the breakdown volume V.

The probability that a cluster will be inside such a volume is determined by the volume density of clusters and the volume V itself. This probability can be found from the Poisson distribution $W = [1 - \exp(-nV)]$, where n is the average density of clusters. In this way the sporadic breakdown regime appears in which, under certain invariable parameters of pulsed laser radiation (the pulse energy and duration, the beam width and divergence) and focusing conditions, the breakdown upon irradiation by a sequence of laser pulses occurs only with some probability $W = N_1/N_0$, where N_1 is the number of breakdown flashes and N_0 is the total number of laser pulses focused to a liquid. For $nV \ll 1$, the probability $W \approx nV \approx N_1/N_0$ and, therefore, the probability N_1/N_0 measured experimentally gives the density $n = (N_1/N_0)V^{-1}$ for a low density of clusters (or a small breakdown volume V).

From the above discussion it follows that, by measuring the breakdown probability, we can estimate the density n of bubston clusters; and by changing some of the liquid parameters (external pressure, temperature, electrolyte concentration, pH), we can measure the dependence of this density on this parameter [25]. Therefore, the breakdown probability rather than the breakdown threshold plays an important role in our measurements. It is obvious that the volume V decreases with decreasing the pulse energy; for a fixed density of clusters, this leads to a decrease in the breakdown probability, resulting finally in the breakdown disappearance.

The optical breakdown is related to a dissolve gas because the density of bubstons and their clusters is determined by the density n_{g}^{s} of a gas dissolved in the liquid. Molecules of this gas, more exactly their solvates (in the case of water, hydrates) play the role of local inhomo-

geneities in the liquid. It is on these solvate inhomogeneities with radii $\Lambda \sim \delta_{liq} + \delta_g$ (where δ_{liq} and δ_g are the radii of molecules of the liquid and dissolved gas, respectively) and density n_g^s that gas cavities (bubston nuclei) can be spontaneously generated during their interaction with dissolved ions involved in thermal (Brownian) motion.

The specific generation rate (per unit volume) of such nuclei is

$$\frac{\delta n_b}{\delta t} \sim d_{eff} D_i n_i n_g^s \exp\left(-\frac{\Delta\varphi}{kT}\right), \quad (1)$$

where n_b is the bubston density; n_i is the density of dissolved ions; D_i is the diffusion coefficient of ions; $\Delta\varphi$ is the minimal increment of the thermodynamic potential of the solution during the formation of a gas cavity of radius r_0; d_{eff} is the coefficient having the dimensionality of length and reflecting a strong dependence of the generation rate on the radii Λ of ions and solvate inhomogeneities and their structure. It is this scale d_{eff} that should be treated as the effective size of inhomogeneities.

Our calculation showed that the nucleus radius for water at a pressure of $p < 10^3$ atm is $r_0 \approx 3$ Å and the corresponding increment is $\Delta\varphi \approx 1$ eV. The generated nuclei grow and pass to a stable state – bubstons with the radius $R \approx 10 - 20$ nm, during diffusion of ions capable of adsorption on their surface and filling of the expanding volume with a dissolved gas. For the specific resistance of water equal to 10 MΩ cm (see below), the Na^+ and Cl^- ions, which are always present in water, have the density $n_i \approx 2\times10^{14}$ cm^{-3}. As the density n_g^s of the dissolved gas increases, the density of bubstons and their clusters also increases. Thus, by varying the dissolved gas concentration, we can control the optical strength of the liquid, while the liquid degassing ($n_g^s \to 0$) allows a complete elimination of the seed mechanism of its breakdown. In this paper, we present the results of measurements of the breakdown probability W of pure water during its degassing.

2. Experimental

2.1 Experimental setup

A cell with a liquid under study mounted on an optical bench was irradiated by laser pulses. The scheme of the experimental setup is shown in Fig. 3. Radiation from single-mode repetitively pulsed Nd^{3+} : YAG laser (*1*) emitting 1.06-μm, 50-ns pulses with a pulse repetition rate of 2 Hz was directed by means of a telescope and a system of lenses to cell (*2*) with a liquid where the optical breakdown was excited. The pulse energy E_L was varied from 10 to 15 mJ. The breakdown appeared at a depth of 5 mm from the liquid surface. Radiation was focused into a spot of diameter 0.5 cm on the cell by a lens with a focal distance of 7.5 cm. Thus, the radiation intensity was varied in our experiments in the range $(0.6 - 0.8) \times 10^9$ W cm^{-2}.

The optical breakdown produced by laser pulses was accompanied by a bright flash and the appearance of a macroscopic cavitation bubble. The method of fixation and study of the cavitation dynamics is well developed (see, for example, [26] and references therein), and the breakdown probability can be simply determined by measuring the probability of appearance of such a bubble. This method is based on the refraction of the probe beam of a cw laser in

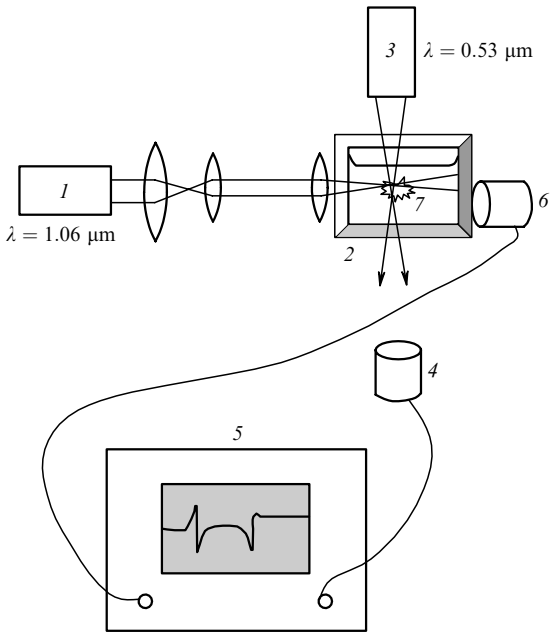

Figure 3. Scheme of the detection of scattered optical radiation and acoustic signal: (*1*) single-mode repetitively pulsed Nd^{3+} : YAG laser; (*2*) cell with liquid; (*3*) frequency-doubled single-mode Nd^{3+} : YAG laser; (*4*) differential photodetector; (*5*) digital oscilloscope; (*6*) piezoelectric sensor; (*7*) flash.

the acoustic wave field appearing first during the optical breakdown and then during the collapse of a cavitation bubble. For this purpose, the breakdown region was irradiated by focused probe 0.53-μm, 40-mW second harmonic radiation from a cw Nd^{3+} : YAG laser (*3*) perpendicular to the first harmonic radiation beam. The beam diameter in the focus did not exceed 50 μm. Note that the mutual location of the probe-beam waist and optical breakdown flash (*7*) was noncritical: the probe beam could be displaced within 5 mm above and below the flash region.

The sound appearing during the breakdown and subsequent collapse of a cavitation bubble modulates the refractive index of water, which causes the deviation of the probe beam from its initial direction. This deviation was measured with differential sensor (*4*) consisting of two photodiodes and sensitive to the probe-beam deviations. The output signal of sensor (*4*) was fed to one of the channels of Tektronix TDS-540 digital store oscilloscope (*5*). Acoustic piezoelectric sensor (*6*) based on a textured piezoelectric film, described in [27], was pressed against the cell. The film thickness was 20 μm and its resonance frequency was 22 MHz. The output signal of this sensor was fed to another channel of the oscilloscope. Thus, we could observe for one laser pulse simultaneously both the signal of scattered probe radiation and acoustic signal. The oscilloscope was triggered by the pulse that triggered the electro-optic gate of a pulsed laser, i.e., synchronously with the laser pulse. The oscilloscope was connected with a computer via a GPIB board for accumulation and digital processing of experimental data. The data array was formed by the output signals of sensors (*4*) and (*6*).

Figure 4 presents oscillograms obtained from a differential photodiode sensor (optical detection channel) and an acoustic sensor (acoustic detection channel). One can see

that in both cases the signal consists of two distinct pulses. The first pulse is caused by the optical breakdown, shock-wave generation, and the appearance of a cavitation bubble. The shock-wave front deflects the probe cw laser beam, resulting in the appearance of a signal on the differential photodiode sensor; the same shock wave also excites the acoustic sensor. It is known that a cavitation bubble formed during optical breakdown first increases, achieving the maximum size, and then collapses. During the collapse, a shock wave is generated, which is detected, as before, with two sensors. One can see that the time interval between pulses in both detection channels is the same, which confirms the validity of the method of parallel detection of the optical breakdown by the probe-beam deflection and by the acoustic pulse.

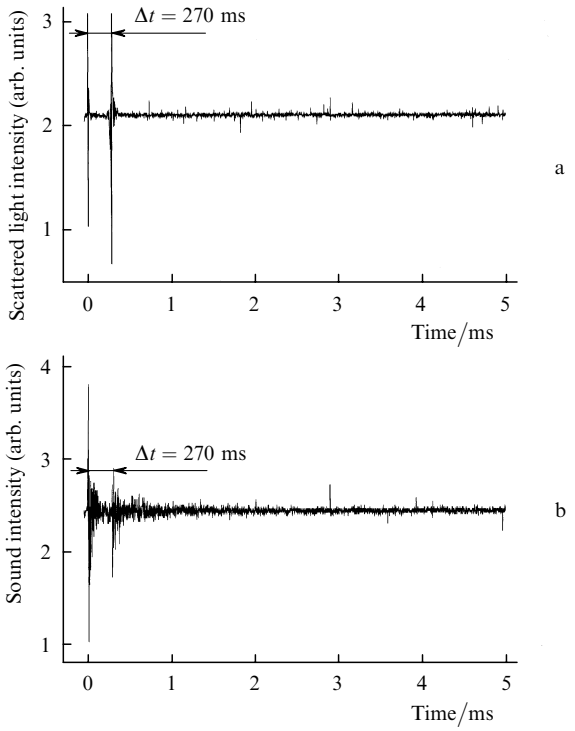

Figure 4. Oscillograms of the optical (a) and acoustic (b) signals.

The data array was processed as follows. The necessary condition was the appearance of two rather intense pulses in both detection channels, which should be divided by the same time interval. This method allows the reliable detection of the breakdown. The breakdown probability was determined from these data in a series of laser shots with a repetition rate of 2 Hz for one minute.

2.2 Preparation of samples

Water was carefully purified in an ion-exchange resin rectification column (the specific resistance was 10 MΩ cm) and poured into a cylindrical Pyrex cell of diameter 40 mm with a vacuum valve. The cell was fabricated by paying a special attention to the elimination of possible contamination sources. For this purpose, the end walls of the cell, through which radiation was coupled and coupled out, were welded, and the vacuum-valve rod was made of Teflon. The cell design allowed the measurements of the resistance and temperature of water with the help of black platinum electrodes located in a Teflon plug and a thermal resistor in a quartz capillary. The cell was filled by half with water. The cell axis was horizontal and the laser beam was parallel to it and was focused at a distance of 5 mm from the water surface. Before water degassing, the water resistance and temperature and the breakdown probability W were measured. Experiments were performed at room temperature in air, argon, helium, and perfluoropropylene (C_3F_6). The main measurements were performed in air, while experiments with the other three gases were additional.

3. Experimental results and discussion

Degassing was performed by stages in the following way. At the first stage, the cell with a free volume filled with air till saturation at the pressure $p = 1$ atm was connected to a backing pump for a minute and a pressure of 10^{-3} Torr was produced in it. Then, the vacuum valve was closed and the resistance and temperature were measured. The temperature measured immediately after pumping out was below the initial temperature, which is explained by the evaporation of water during pumping out, while the resistance values had a large scatter. This is probably explained by the fact that the electrode surface is covered with bubbles (which can be observed with a microscope). After 10–15 min, the temperature and resistance acquired the initial values. Then, the cell settled for 24 hours; during this time, a free volume was filled with the equilibrium water vapour and the excess dissolved gas that has escaped from water. After 24 hours, the pressure p in a free volume and the probability W were measured. The second and next stages also began from pumping out a free volume with a backing pump for a minute followed by the cell sealing and settling for 24 hours. At the end of each stage, the pressure p and probability W were measured, whose dependences on the number N of the degassing stage are presented in Fig. 5.

One can see from Fig. 5a that the residual gas pressure p decreases with increasing N, reaching the stationary level at the third-fourth stage, which corresponds to the saturated vapour pressure at room temperature $p_{sat} = 17.5$ Torr. The fact that such a stationary residual pressure $p = p_{sat}$ is achieved within 75–100 h after the beginning of degassing agrees with the quantitative estimate of the diffusion time τ_d of dissolved nitrogen from the water volume having the maximum depth $h \approx 20$ mm (half the cell diameter): $\tau_d \sim h^2/D \approx 85$ h (where $D \approx 1.3 \times 10^{-5}$ cm^2 s^{-1} is the tabulated value of the diffusion coefficient of nitrogen molecules in water at room temperature).

The establishment of the stationary pressure $p = p_{sat}$ does not mean, of course, that water becomes completely degassed. The hydrates of a dissolved gas with anomalously long lifetimes can be preserved in water with some probability; in other words, a part of dissolved gas molecules can be in potential traps with long lifetimes. This assumption is indirectly confirmed by measurements of the breakdown probability W presented in Fig. 5b. One can see that, as N increases, the probability W first decreases together with a decrease in the pressure p, but for $N = 4$, when p becomes close to p_{sat}, it drastically increases, remaining high as N further increases. This is explained by the fact that for $p = p_{sat}$, water is at the boiling point, and vapour bubbles are vigorously formed on hydrate inhomogeneities remained in water, at which the optical breakdown occurs.

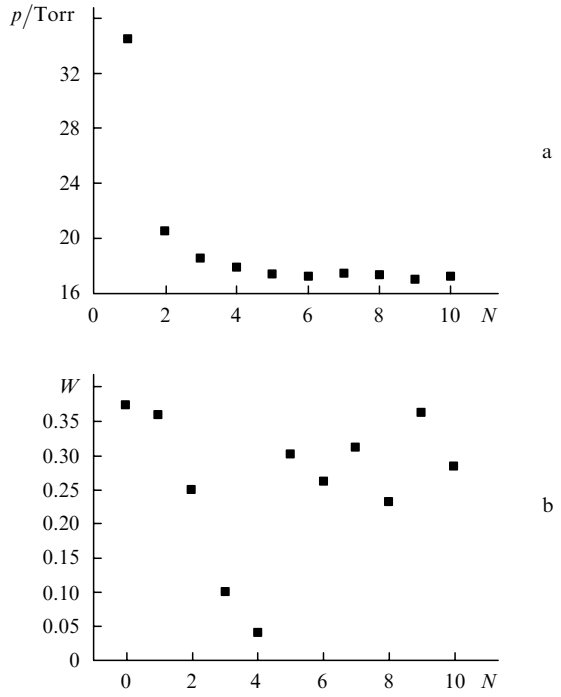

Figure 5. Dependences of the residual pressure p in a cell (a) and the optical breakdown probability W (b) on the degassing stage number N. The value $W(0)$ corresponds to the optical breakdown probability measured under normal conditions (the point $p(0)$ is absent in Fig. 5a).

In this case, the picture of the breakdown flash differs from that observed under normal conditions. Figure 6 shows the photographs of two such pictures. One can see that when $p = p_{sat}$, the flash is surrounded by a halo, which is observed if a light background exists in the laboratory; and no halo is observed in the completely darkened room. Note also that for $p = p_{sat}$, the time interval between the first and second pulses (see Fig. 4) is 5–6 times longer than that at the atmospheric pressure. Because, as shown above, this interval is the interval between the appearance and collapse of a cavitation bubble (i.e., it is in fact the lifetime of the bubble), we may say that, when $p = p_{sat}$, the lifetime of the cavitation bubble is longer and as a consequence its size achieves approximately one centimetre.

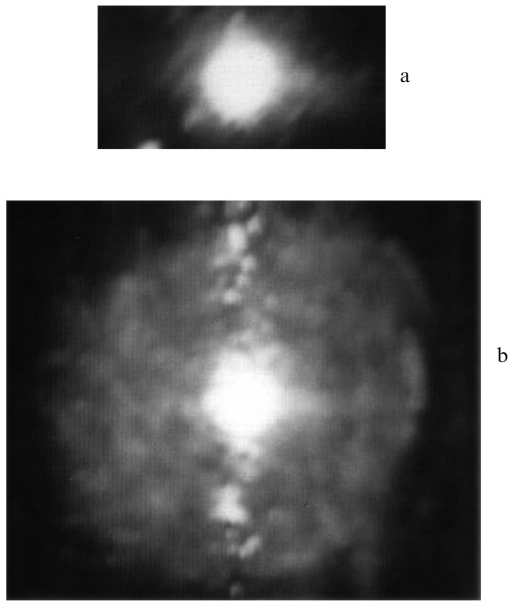

Figure 6. Characteristic view of the optical breakdown flash obtained under normal conditions (a) and for $p \simeq p_{sat}$ (b). The halo around the breakdown flash is observed.

Thus, we can assert that the flash halo is caused by scattering of the background light from a cavitation vapour–gas bubble whose radius at $p = p_{sat}$ considerably exceeds that under normal conditions. The 'vapour' origin of the breakdown at $p = p_{sat}$ was also confirmed in another experiment. A cell with pure water open to atmosphere was connected to a liquid thermostat, and the temperature dependence of the breakdown probability W was measured (Fig. 7). One can see from Fig. 7 that the probability W weakly depends on temperature up to $T = 97\,^{\circ}\mathrm{C}$. As the temperature T was further increased, we observed a strong dependence $W(T)$ and flashes surrounded by a halo.

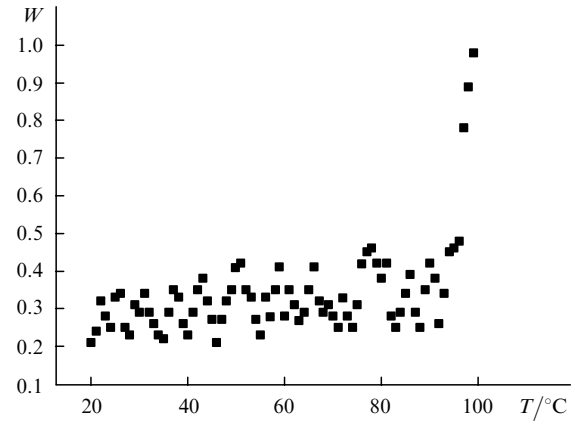

Figure 7. Temperature dependence of the optical breakdown probability W.

The assumption about the existence of long-lived hydrates of a dissolve gas stimulated our additional experiments with the aim to find the dependence of this hypothetical effect on the type of a gas. In the first experiment, we pumped helium at a pressure of 5 atm into a free volume of a cell with preliminary degassed water (by the method described above). After 120 hours of settling and obtaining a saturated solution, the above-described degassing procedure was used. The results of measuring the residual pressure p and breakdown probability W presented in Fig. 8 show that the stationary pressure $p = p_{sat}$ is established as in air, whereas the breakdown probability W monotonically tends to zero with increasing N. For $N \geqslant 4$ (when $p = p_{sat}$), we have failed to obtain breakdown even at radiation intensities up to 10^{12} W cm^{-2}. Thus, this experiment showed that helium can purify ('wash') water from long-lived hydrates of air dissolved in it (to remove air molecules from traps). A cell with water cleaned by helium was placed into a thermostat and heated to 100 °C; no boiling was observed in this case and breakdown was still absent. Such water proves to be also insensitive to mechanical perturbations such as shaking and stirring.

We tested the property of helium to 'wash' water from long-lived hydrates of gases dissolved in it with two other

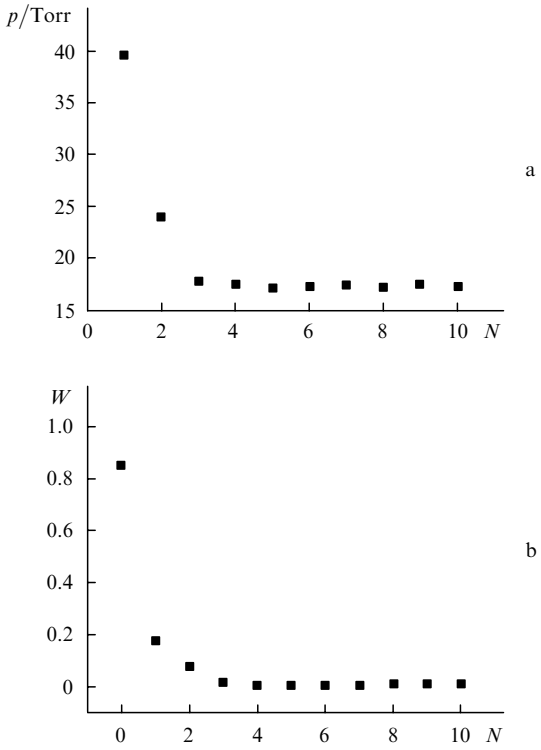

Figure 8. Dependences of the residual pressure in a cell (a) and the optical breakdown probability W (b) on the degassing stage number N when the helium 'washing' was used. The value $W(0)$ corresponds to the optical breakdown probability for $p = 5$ atm (the point $p(0)$ is absent in Fig. 5a).

gases: argon and perfluoropropylene. Water preliminary 'washed' with helium and then saturated (for a week) by these gases at a pressure of 1 atm and temperature 20 °C was degassed by the above-described method. Note that, according to the reference data, perfluoropropylene is insoluble in water. However, in fact the solubility of perfluoropropylene in water, which we measured by the residual pressure after a week settling in a sealed cell, was $s = 3$ ml/100 g (for argon, our measurements gave the value $s = 8$ ml/100 g). The dependences of the pressure p and the probability W on the stage number N measured for both gases were qualitatively close to those obtain for air and are not presented here. At the same time, there exists a noticeable difference between the use of argon and perfluoropropylene, which consist in the fact that for all residual pressures $p > p_{sat}$, the breakdown probability W for perfluoropropylene is considerably higher (by several times) than that for argon (for $p \approx p_{sat}$, when the breakdown occurs on vapour bubbles, the probabilities W for these gases are comparable).

This fact proves to be unexpected within the framework of our seed mechanism of breakdown considered above. According to this mechanism, the solubility of perfluoropropylene is approximately three times lower than that of argon and, therefore, the breakdown probability W for perfluoroperylene should be lower (rather than a few times high, as in experiments) than that for argon.

The unusual behaviour of perfluoroperylene was also observed upon washing water solutions of argon and perfluoropropylene by helium by the method described above. We have managed to suppress the breakdown in water preliminary saturated with argon, whereas, when perfluoropropylene was used, we have failed to do it even after triple washing. This feature of the behaviour of perfluoropropylene during the optical breakdown shows that the seed breakdown mechanism presented above requires the refinement in the case of water solutions of 'giant' (in size and mass) molecules such as perfluoropropylene. It seems that the above-introduced concept of local solvate (hydrate) inhomogeneities on which bubston nuclei can be created should be considerably refined to take into account not only their radii $\Lambda \sim \delta_{liq} + \delta_g$ and structures but also other properties playing a noticeable role in the seed formation. One can expect that such an approach applied to 'giant' molecules will lead to the mesoscopic values of the effective sizes d_{eff} of inhomogeneities (of the order of a few nanometres and more). Then, according to (1), low concentrations of a dissolved gas in the case of such molecules can be compensated by the 'giant' values of d_{eff}.

4. Conclusions

Thus, we believe that our experiments have proved that the optical breakdown in water is initiated by a gas dissolved in it due to the formation of bubston clusters. It seems that we have managed to obtain for the first time completely degassed water free of bubstons and any other evaporation seeds. The optical breakdown in such water caused by the seed mechanism is absent both away and near the boiling point. The suppression of the optical breakdown is achieved by using the ability of helium to purify ('wash') water from long-lived hydrates of other gasses dissolved in water (except such as perfluoropropylene), which we have discovered. The existence of such long-lived hydrates has been also found in our paper; however, the study of the physics of this phenomenon and the role of dissolved helium remain outside the scope of our investigation.

It should be noted once more that the optical breakdown effect under study concerns only its seed mechanism with the threshold intensities $I_{th} \sim 10^{10}$ W cm^{-2}. Of course, completely degassed pure water (as any other dielectric liquid) has the limiting optical damage threshold, which is determined by the multiphoton ionisation of its molecules. In this case, the threshold breakdown intensities exceed the breakdown threshold of water containing a dissolved gas. However, this is another field of phenomena, which we do not consider here.

Acknowledgements. This work was supported by the Russian Foundation for Basic Research (Grant No. 05-02-08311) and the Foundation for Support of the Russian Science.

References

1. Lyamshev L.M. *Usp. Fiz. Nauk*, **135**, 637 (1981).
2. Butenin A.V., Kogan B.Ya. *Kvantovaya Elektron.*, (5), 143 (1971) [*Sov. J. Quantum Electron.*, 1, 561 (1971)].
3. Bunkin N.F., Kuseleva O.A., Lobeyev A.V., Movhan T.G., Ninham B.W., Vinogradova O.I. *Langmuir*, 13, 3024 (1997).
4. Kennedy P.K., Hammer D.X., Rockwell B.A., in *Prog. in Quantum Electron.* (Amsterdam: Elsevier Science Ltd, 1997) Vol. 21, No 3, pp 155 – 248.
5. Grand D., Bernas A., Amouyal E. *Chem. Phys.*, 44, 73 (1979).
6. Williams F., Varma S.P., Hillenius S. *J. Chem. Phys.*, **64**, 1549 (1976).
7. Keldysh L.V. *Zh. Eksp. Teor. Fiz.*, **47**, 1945 (1965).

8. Baltuška A. *Hydrated Electron Dynamics Explored with 5-fs Optical Pulses* (Rijksuniversiteit Groningen, Netherlands, Proefschrift, 2000) p. 160.
9. Liu W., Kosareva O., Golubtsov I.S., Iwasaki A., Becker A., Kandidov V.P., Chin S.L. *Appl. Phys. B*, **76**, 215 (2003).
10. Raizer Yu.P. *Lazernaya iskra i rasprostranenie razryadov* (Laser Spark and Propagation of Discharges) (Moscow: Nauka, 1974).
11. Bunkin N.F., Bunkin F.V. *Zh. Eksp. Teor. Fiz.*, **100**, 512 (1992).
12. Bunkin N.F., Bunkin F.V. *Zs. Phys. Chem.*, **111**, 215 (2001).
13. Bunkin N.F., Bunkin F.V. *Zh. Eksp. Teor. Fiz.*, **123**, 828 (2003).
14. Bunkin N.F., Vinogradova O.I., Kuklin A.I., Lobeev A.V., Movchan T.G. *Pis'ma Zh. Eksp. Teor. Fiz.*, **62**, 660 (1995).
15. Bunkin N.F., Lobeyev A.V., Lyakhov G.A., Ninham B.W. *Phys. Rev. E*, **60**, 1681 (1999).
16. Bunkin N.F., Karpov V.B. *Pis'ma Zh. Eksp. Teor. Fiz.*, **52**, 669 (1990).
17. Sankin G.N., Teslenko V.S. *Dokl. Ross. Akad. Nauk*, **393** 762 (2003).
18. Bunkin N.F., Lobeyev A.V. *Phys. Lett. A*, **229**, 327 (1997).
19. Bunkin N.F., Lobeev A.V. *Pis'ma Zh. Eksp. Teor. Fiz.*, **58**, 91 (1993).
20. Bunkin N.F., Suyazov N.V., Tsipenyuk D.Yu. *Kvantovaya Elektron.*, **35**, 180 (2005) [*Quantum Electron.*, **35**, 180 (2005)].
21. Bunkin N.F., Bunkin F.V. *Laser Phys.*, **3**, 63 (1993).
22. Bunkin N.F., Lobeev A.V. *Pis'ma Zh. Tekh. Fiz.*, **19**, 38 (1993).
23. Bunkin N.F., Lobeev A.V. *Kvantovaya Elektron.*, **21**, 319 (1994) [*Quantum Electron.*, **24**, 297 (1994)].
24. Vinogradova O.I., Bunkin N.F., Churaev N.V., Kiseleva O.A., Lobeyev A.V., Ninham B.W. *J. Col. Int. Sci.*, **173**, 443 (1995).
25. Bunkin N.F., Lobeyev A.V., Mikhalevich V.G. *Phys. Vibrations*, **7**, 205 (1999).
26. Vogel A., Lauterborn W. *Appl. Opt.*, **27**, 1869 (1988).
27. Veselovskii I.A., Dorozhkin L.M., Lazarev V.V., Mikhalevich V.G., Pleshkov G.M., Rodin A.M., Chayanov B.A. *Akoust. Zh.*, **33**, 834 (1987).